ACS OMEGA

Article

Cite This: ACS Omega 2018, 3, 6182−6189

Development of Magnetic Nanocomposite Hydrogel with Potential Cartilage Tissue Engineering

Jianghong Huang,[†,‡,§] Yujie Liang,[∥,⊥] ZhaoFeng Jia,[†,‡,§] Jielin Chen,[†,‡,§] Li Duan,[†,‡,§] Wei Liu,[†,‡,§] Feiyan Zhu,[†,‡,§] Qian Liang,[†,‡,§] Weimin Zhu,[†,‡,§] Wei You,[†,‡,§] Jianyi Xiong,*[,†,‡,§] and Daping Wang*[,†,‡,§]

[†]Shenzhen National Key Department of Orthopedics, [‡]Shenzhen Key Laboratory of Tissue Engineering, and [§]Shenzhen Laboratory of Digital Orthopedic Engineering, Shenzhen Second People's Hospital (The First Hospital Affiliated to Shenzhen University), Shenzhen 518035, China

[∥]Shenzhen Institute of Mental Health, Shenzhen Mental Health Center, Shenzhen Kangning Hospital, Shenzhen 518020, Guangdong Province, China

[⊥]Departments of Chemistry, The Chinese University of Hong Kong, Shatin 999077, Hong Kong SAR, China

ABSTRACT: Magnetic nanocomposite hydrogels show high potential to improve tissue engineering. In this study, a magnetic nanocomposite hydrogel was prepared from poly(vinyl alcohol), nano-hydroxyapatite (n-HA), and magnetic nanoparticles (Fe_2O_3) using the ultrasonic dispersion method and freeze−thaw cross-linking molding. The water content and crystallinity of the magnetic nanocomposite hydrogel were tested. Microscopic morphology assessment, mechanical testing, and characterization were performed. Additionally, the magnetic nanocomposite hydrogel was co-cultured with bone mesenchymal stem cells (BMSCs) to determine its cell compatibility. We found that the magnetic nanocomposite hydrogel had good mechanical properties and that its mechanical properties were enhanced by the addition of n-HA. The BMSCs showed uniform growth on the surface of the magnetic nanocomposite hydrogel and high rates of proliferation. BMSC growth was also enhanced by the addition of Fe_2O_3 and also significant stimulated chondrocyte-related gene expression. Thus, the magnetic nanocomposite hydrogel scaffold material we describe here could have broad applications in cartilage tissue engineering.

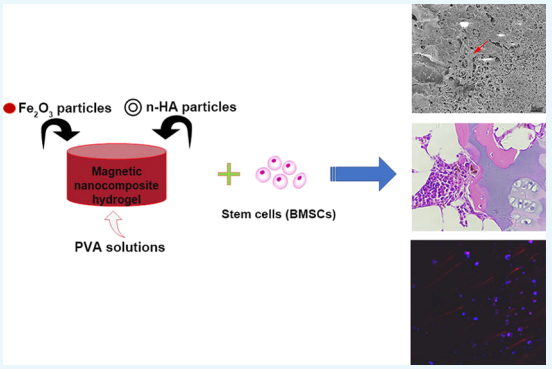

1. INTRODUCTION

Articular cartilage defects are one of the most common forms of orthopedic disease and are challenging to treat in the clinic. Articular cartilage must be replaced after injury or lesion because it has limited ability to self-repair. The emergence of bioengineered cartilage brings hope for patients with articular cartilage defects. Tissue engineering of cartilage requires an appropriate scaffold material, which cannot only temporarily replace or repair the tissue but also provides a growth environment for seed cells. The chemical composition and the physical structure of the scaffold material affect the rate of cell proliferation and differentiation, as well as maintenance of cell phenotype.[1] Injectable hydrogel is a scaffold material with the capacity to self-model, which can be used to fill tissue defects of different shapes and sizes, with minimal trauma. Cells can distribute uniformly in a hydrogel scaffold and grow in three dimensions. Hydrogel provides a bionic environment,[2] and its high water content supports the exchange of nutrients and cellular metabolites. poly(vinyl alcohol) (PVA) hydrogel, a water-soluble polymer that is hydrolyzed from polyvinyl acetate, is prepared using the repeated freeze−thaw cross-linking molding process. With high water content, high water absorption, excellent biocompatibility, flexibility, and high elasticity, it can substantially reduce the stimulation of cells and tissues. Additionally, when the damaged articular surface repaired with PVA hydrogel to form a neocartilage tissue could resemble the native cartilage, it is an ideal artificial cartilage implant material.[3,4]

Nano-hydroxyapatite (n-HA) has excellent biological activity, good biocompatibility, and bone conductivity because its chemical composition and crystal structure are similar to the inorganic component of the natural bone. The addition of HA could enhance the mechanical properties of scaffolds, which provide a template for a covering chondrocyte suspension and render the scaffolds sufficient integration with the host tissue to protected subchondral bone regeneration. Magnetic nanoparticles (Fe_2O_3) can promote the proliferation and differentiation of bone mesenchymal stem cells (BMSCs). Previous studies have integrated Fe_2O_3 into a porous scaffold to create a magnetic scaffold and found enhanced proliferation and adhesion of BMSCs in vitro.[5] It is reported that labeling BMSCs with Fe_2O_3 causes cells to transfer from the

Received: February 19, 2018
Accepted: April 19, 2018
Published: June 8, 2018

DOI: 10.1021/acsomega.8b00291
ACS Omega 2018, 3, 6182−6189

extracellular matrix to the sites of cartilage damage, which promotes the differentiation of BMSCs into cartilages and stimulates chondrogenesis.[6,7] Previous findings by Ngadiman et al.[8,9] and Sheikh et al.[10] have shown the biocompatibilities of Fe_2O_3/PVA and n-HA/PVA, and they are recommended to execute a side-by-side study comparing the proliferation and the differentiation of cells when they are seeded on PVA, Fe_2O_3/PVA, n-HA/PVA, and n-HA/Fe_2O_3/PVA.[11,12]

In this study, we prepared a magnetic nanocomposite hydrogel using PVA, n-HA, and Fe_2O_3. We found that the Fe_2O_3 regulated cell behavior within the scaffold material and had good cell compatibility; thus, they were used to construct tissue-engineered cartilage in vitro.

2. MATERIALS AND METHODS

2.1. Reagents and Instruments. The following reagents and instruments were used in this study: PVA, n-HA, Fe_2O_3 (Shenzhen Xincheng Biotechnology Co., Ltd.), Dulbecco's modified Eagle's medium (DMEM), trypsin, fetal bovine serum (FBS), 500 U/mL penicillin and 500 μg/mL streptomycin (Gibco USA), phosphate buffer solution (PBS), Cell Counting Kit-8 (CCK-8) (Keygen Tec), ultrasonic oscillator, weight meter, magnetic stirrer (Central Laboratory of The Second People's Hospital of Shenzhen), differential scanning calorimeter (DSC) (Shenzhen Polytechnic), mechanical tester CTM4000 (Research Institute of Tsinghua University in Shenzhen), and electronic microscope (MIRA3 TESCAN, Research Institute of Tsinghua University in Shenzhen).

2.2. Preparation of Magnetic Nanocomposite Hydrogel. Figure 1 presents the schematic illustration of the fabrication of n-HA/Fe_2O_3/PVA hybrid magnetic nanocomposite hydrogel. Briefly, n-HA, Fe_2O_3, and PVA in a ratio of 1:0.5:10 were mixed and dissolved in deionized distilled water to produce Fe_2O_3. The n-HA/Fe_2O_3/PVA composite hydrogel was successfully prepared using the ultrasonic dispersion method and freeze-thawing cross-linking molding process. To create PVA aqueous solutions, varying amounts of PVA were weighed and placed in distilled water and heated and stirred at 90 °C for 1 h, to fully dissolve the PVA. Varying quantities of n-HA particles and Fe_2O_3 were added into the PVA aqueous solution; after ultrasonic treatment, the solution was stirred at 60 °C until evenly mixed. Next, after 30 min of heat preservation, all the bubbles in the solution were removed with a needle tube. The solution was poured into a mold, and then the mold was placed in the freezer (−20 °C) overnight for 16 h. Next, the solution was removed and thawed at room temperature for 4 h. Repeated freezing and thawing were performed seven times to obtain the n-HA/Fe_2O_3/PVA composite hydrogel (Figure 2A). The prepared n-HA/Fe_2O_3/PVA composite hydrogel was immersed in distilled water for one day to remove non-cross-linked monomers. As a control, we also concurrently prepared a pure PVA hydrogel (Figure 2B).

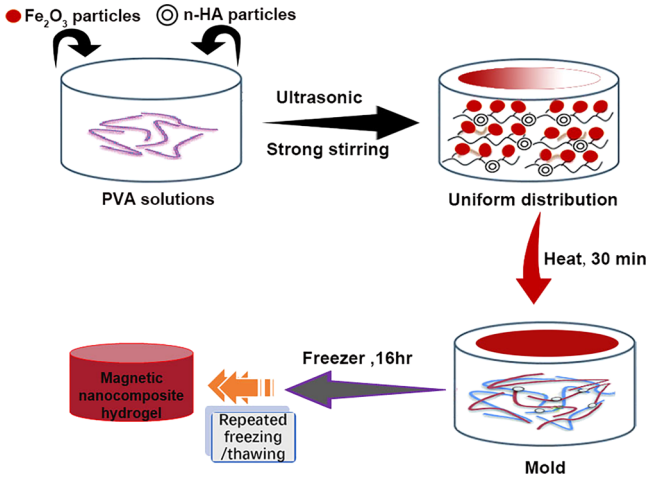

Figure 1. General scheme of the fabrication of n-HA/Fe_2O_3/PVA hybrid magnetic nanocomposite hydrogel.

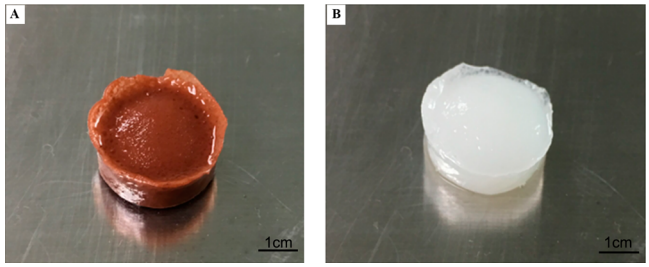

Figure 2. General view of the hydrogel material. (A) n-HA/Fe_2O_3/PVA composite hydrogel and (B) the pure PVA hydrogel.

2.3. Water Content and Crystallinity of the Magnetic Nanocomposite Hydrogel. *2.3.1. Determination of Water Content of the Magnetic Nanocomposite Hydrogel.* The surface water of the magnetic nanocomposite hydrogel was gently dried with a piece of filter paper and placed into a dry beaker of known mass (m_2). By weighing with a scale, the total mass of the hydrogel with beaker was m_3, and the mass of the magnetic nanocomposite hydrogel was calculated as $m_1 = (m_3 - m_2)$. The magnetic nanocomposite hydrogel was placed in a vacuum-drying oven and was dried at 60 °C for 36 h, until it reached a constant weight. The mass of the dried magnetic nanocomposite hydrogel was m_0, and the water content of the dried magnetic nanocomposite hydrogel was determined as $W = (m_1 - m_0)/m_1$.

2.3.2. Test of Magnetic Nanocomposite Hydrogel Crystallinity. The magnetic nanocomposite hydrogel was placed in a vacuum-drying oven and then dried at 60 °C for 24 h until a dried magnetic nanocomposite hydrogel was obtained. About 5 mg of the dried magnetic nanocomposite hydrogel (precision: 0.01 mg) was accurately weighed with a microbalance and placed in an aluminum crucible with a hole in the cover and then was measured with a DSC. An empty crucible of the same type was used as a control. High-purity nitrogen (volume fraction: 0.99999) was used as a protective gas and a purge gas, with a respective flow rate of 20 and 70 mL·min^{-1}. The temperature of the DSC was elevated from 10 °C/min to 250 °C using the programmed temperature to obtain the melting enthalpy of the dried magnetic nanocomposite hydrogel. This value was then used to calculate the crystallinity of the dried magnetic nanocomposite hydrogel.

2.4. Characterization of Hydrolytic Degradation. The weight loss method was used for the characterization of the hydrogel degradation performance in PBS. In this experiment, the same qualities of n-HA/Fe_2O_3/PVA hydrogel and pure PVA hydrogel were suspended in a PBS (pH 7.5) incubator at 37 °C for degradation experiments. At the selected time points (0, 2, 4, 6, 8, 10, 12, 14, 16, 18, 20 days), the qualities of the hydrogels in each group were measured.

DOI: 10.1021/acsomega.8b00291
ACS Omega 2018, 3, 6182−6189

Table 1. Primer Sequences for Real-Time PCR Analysis

genes	forward primer (5′−3′)	reverse primer (5′−3′)
SOX-9	GACGTGCAAGCTGGGAAA	CGGCAGGTATTGGTCAAACTC
Col2A1	CGCCACGGTCCTACAATGTC	GTCACCTCTGGGTCCTTGTTCAC
AGG	GCTACACCCTAAAGCCACTGCT	CGTAGTGCTCCTCATGGTCATC
GAPDH	GGCACAGTCAAGGCTGAGAATG	ATGGTGGTGAAGACGCCAGT

2.5. Mechanical Testing and Microscopic Morphology Analysis. *2.5.1. Mechanical Testing.* The elastic modulus measurement of the n-HA/Fe_2O_3/PVA composite hydrogel was characterized using an electronic universal testing machine CTM4000 in the mechanical testing laboratory. The diameter, thickness, and loading rate of the n-HA/Fe_2O_3/PVA composite hydrogel were 5 mm, 3 mm, and 5.00 mm/min, respectively.

2.5.2. Microscopic Morphology Analysis. The n-HA/Fe_2O_3/PVA composite hydrogel was frozen and dried. Next, after metal spraying, scanning analysis of the surface and cross section of the n-HA/Fe_2O_3/PVA composite hydrogel were conducted. The microscopic morphology of the n-HA/Fe_2O_3/PVA composite hydrogel was observed and analyzed using a TESCAN (Czech Republic) field emission scanning electron microscope. We acquired secondary electron images and backscattered electron images.

2.6. Cell Culture and Cell Compatibility Study. A New Zealand white rabbit (aged 3 months) was anesthetized and then underwent skin disinfection and preparation. The rabbit's bone marrow was punctured at the left femur trochanter, and about 3 mL of bone marrow was extracted using a syringe containing 2 mL heparin. The extracted bone marrow was placed into a 10 mL centrifuge tube, and the PBS was added to reach 5 mL. The bone marrow solution was centrifuged at 1200 rpm for 10 min, and the supernatant was discarded. The pellet was washed twice with PBS, followed by centrifugation at 1000 rpm. High-glucose DMEM culture solution (containing 10% FBS, 1% double-antibody penicillin/streptomycin) (5 mL) was added to the precipitated cell suspension, and then the mixed solution was cultured in a CO_2 incubator at 5% CO_2 and 37 °C. Three days after culture, fresh medium was added to the flasks. Cells were digested with 0.25% (w/v) trypsin and 0.02% (w/v) ethylenediaminetetraacetic acid (Hyclone, USA) and subcultured at a density of 1.0×10^4 cells/cm^2. The BMSCs of passage 3 were co-cultured with the n-HA/Fe_2O_3/PVA composite hydrogel for cell compatibility study, and the cell compatibility of the composite material was observed (Figure 5A,B). For chondrogenic differentiation experiment, we used serum-free chondrogenic medium, which consisted of DMEM (4.5 g/L glucose; Biochrom), 1% Insulin-transferrin-selenium (ITS) supplement, 100 nM dexamethasone, 0.17 mM L-ascorbic acid-2-phosphate, 1 mM sodium pyruvate, and 0.35 mM L-prolin (all from Sigma-Aldrich, USA).

2.6.1. Cell Proliferation Assay. Cell proliferation was measured using the CCK-8 method. This experiment analyzed three groups: BMSCs co-cultured with n-HA/Fe_2O_3/PVA composite hydrogel (group A), BMSCs co-cultured with pure PVA hydrogel (group B), and BMSCs cultured alone (group C), with five repeat samples in each group. Cells at the exponential phase were seeded in 96-well plates at a density of 1×10^3 cells per well. On the first, third, fifth, seventh, and ninth days of cell culture, 50 μL CCK-8 solution was added to each complex hole and then incubated at 37 °C for 4 h. Next, the solution in each complex hole was transferred to a 96-well plate, and the amount of solution in each well was equalized. Light absorption values (*A* value, 490 nm wavelength) were measured with a Thermo-plate microplate reader (Rayto Life and Analytical Science Co., Ltd., Germany) and were used to create a cell proliferation curve.

2.6.2. Stereoscopic Optical Microscopy. This experiment examined two groups: BMSCs cultured with n-HA/Fe_2O_3/PVA composite hydrogel (group A) and BMSCs cultured with pure PVA hydrogel (group B). The culture plate was uncovered after one week of culture and placed under a stereoptical microscope. A 100× magnification was used to observe cell growth.

2.6.3. Scanning Electron Microscopy. This experiment examined two groups: BMSCs cultured with n-HA/Fe_2O_3/PVA composite hydrogel (group A) and BMSCs cultured with pure PVA hydrogel (group B). After one week of culture, the hydrogels in each group were washed twice with PBS, fixed with 2.5% glutaraldehyde fixative at 4 °C for 2 h, and then dehydrated progressively with ethanol. After critical-point drying with CO_2 and metal spraying, the adhesion of cells on the scaffold was observed with a scanning electron microscope.

2.7. Histological and Immunohistochemical Analyses to Detect the Collage Protein. For histology, the cell/scaffold constructs were fixed in 2.5% glutaraldehyde for 16 h, through a series of gradient ethanol to dehydrate, embedded in paraffin wax, and cut into 5 μm thick sections, and then the samples were stained with hematoxylin and eosin (H&E). For immunofluorescent staining to detect the collage II protein expression levels, the cell/scaffold constructs were fixed with 4% paraformaldehyde for 10 min, permeabilized with 0.25% Triton X-100 for 10 min, and then blocked with 3% bovine serum albumin for 60 min. Subsequently, these constructs were incubated with a collagen type II antibody (ab34712, 1:100, Abcam, Cambridge, USA) and then were subsequently exposed to Alexa Fluor 594-conjugated secondary antibody overnight. Nuclei were counterstained with 4′,6-diamidino-2-phenylindole (DAPI) and are shown in blue. The constructs were cut into thick sections and were visualized using laser-scanning confocal microscopy (ZEISS, Germany).

2.8. RNA Extraction and Real-Time Polymerase Chain Reaction Analysis. Total RNA was isolated using Trizol and reverse-transcribed into complementary DNA using a DNA synthesis kit (TaKaRa, Shiga, Japan) according to the manufacturer's protocol. Real-time polymerase chain reactions (PCRs) of glyceraldehyde phosphate dehydrogenase (GAPDH), collagen II, and aggrecan were performed using the SYBR Green QPCR Master Mix. Primer sequences are listed in Table 1. Real-time PCRs were performed using a 7500 real-time PCR detection system (ABI, Foster City, CA) at 95 °C for 15 min followed by 40 cycles of denaturation at 95 °C for 10 s, extension at 60 °C for 15 s, and annealing at 72 °C for 15 s. Gene expression levels were normalized to the housekeeping gene GAPDH, and the relative gene expression was calculated using the ΔΔCT method.

DOI: 10.1021/acsomega.8b00291
ACS Omega 2018, 3, 6182−6189

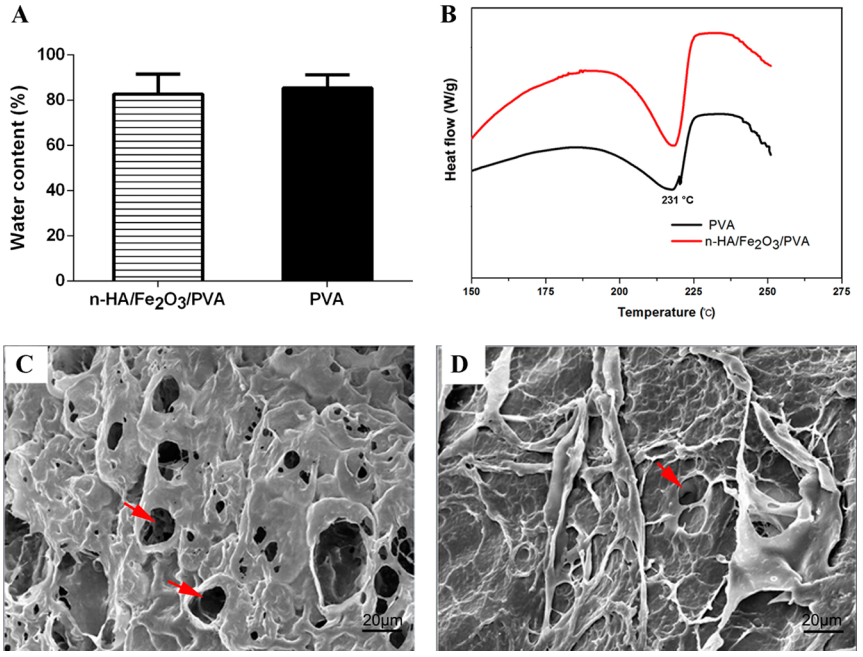

Figure 3. (A) Water contents of the n-HA/Fe_2O_3/PVA hydrogel and the pure PVA hydrogel. (B) DSC atlas of the dried n-HA/Fe_2O_3/PVA composite hydrogel and the dried pure PVA hydrogel. (C) Scanning electron microscopic image of the n-HA/Fe_2O_3/PVA composite hydrogel (2000×). (D) Scanning electron microscopic image of the pure PVA hydrogel (2000×).

3. RESULTS AND DISCUSSION

3.1. Water Content and Crystallinity of the Magnetic Nanocomposite Hydrogel. *3.1.1. Water Content of the Magnetic Nanocomposite Hydrogel.* The water content of the novel magnetic nanocomposite hydrogel we prepared was 82.6%, lower than the water content of the pure PVA hydrogel (85.3%, Figure 3A). This phenomenon could be explained as follows: PVA was closely linked with n-HA and Fe_2O_3, producing stress shrinkage, causing molecules to become densely packed, forcing water in the pores to be discharged, and decreasing the volume of the magnetic nanocomposite hydrogel. Consequently, the hydroxyl of water molecule-producing hydrogen bond left little space to accommodate water molecules, which resulted in lower water content.

3.1.2. Crystallinity of the Magnetic Nanocomposite Hydrogel. Scaffolds with high crystallinity can have a high elastic modulus and elongation at break.[13] Changes to the crystallinity of the dried magnetic nanocomposite hydrogel could indirectly suggest that its structure has changed. It was believed that a polymer's crystallinity is proportional to its melting heat when melted.

The melting heat can be measured using DSC atlas. Figure 3B shows the DSC atlas of the dried n-HA/Fe_2O_3/PVA composite hydrogel and the DSC atlas of the dried pure PVA hydrogel. As shown in Figure 3B, the dried n-HA/Fe_2O_3/PVA composite hydrogel showed a sharp endothermic peak around 217 °C, corresponding to its melting heat, and showed a wide endothermic peak at 231 °C, corresponding to its decomposition. The dried pure PVA hydrogel showed a sharp endothermic peak around 221 °C, corresponding to its melting heat, and showed a wide endothermic peak at 236 °C, corresponding to its decomposition. By comparing to previously reported values of the melting heat of 100% crystallized PVA, the crystallinity of the hydrogel samples was obtained using the following equation[14]

$$f(\mathrm{DSC}) = (\Delta H/\Delta H^0) \times 100\%$$

where f(DSC) is the crystallinity of the hydrogel samples measured through differential thermal analysis, ΔH is the melting heat enthalpy of the hydrogel samples, and ΔH^0 is the melting heat enthalpy of the PVA hydrogel with 100% crystallinity, reported to be 138.6 J/g.[15] Table 2 shows the melting heat enthalpies of the dried n-HA/Fe_2O_3/PVA composite hydrogel and the dried pure PVA hydrogel and their crystallinities as calculated using the formula above.

Table 2. Melting Heat Enthalpies of the Dried n-HA/Fe_2O_3/PVA Composite Hydrogel and the Dried Pure PVA Hydrogel (n = 10)

name of the hydrogel	T/°C	ΔH/J·g^{-1}	f(DSC)
the dried n-HA/Fe_2O_3/PVA composite hydrogel	217	52.7 ± 7.1	38.02 ± 4.5
the dried pure PVA hydrogel	221	59.6 ± 6.8	43.01 ± 3.2

3.2. Microscopic Morphology Analysis. The scanning electron microscopy (SEM) showed that many pores of different sizes were distributed on the surface of the magnetic nanocomposite hydrogel and that magnetic particles and n-HA particles were uniformly distributed in the magnetic nanocomposite hydrogel, forming rough bumps on the surface. These pores and bumps were beneficial to the adhesion and growth of cells on the surface of the magnetic nanocomposite hydrogel. In contrast, relatively few pores were distributed on the surface of the pure PVA hydrogel (Figure 3C,D).

3.3. Mechanical Property and the Degradation Testing. The mechanical properties of the hydrogel samples were detected by a three-point bending resistance experiment. The results showed that the n-HA/Fe_2O_3/PVA composite hydrogel had better mechanical properties than the pure PVA hydrogel, including greater tensile strength, greater bending strength, and a higher bending modulus (as shown in Table 3). The in vitro

DOI: 10.1021/acsomega.8b00291
ACS Omega 2018, 3, 6182−6189

Table 3. Mechanical Properties of the n-HA/Fe_2O_3/PVA Composite Hydrogel and the Pure PVA Hydrogel ($\bar{x} \pm s$, n = 10)

name of the hydrogel	tensile strength (MPa)	bending strength (MPa)	bending modulus (GPa)
the n-HA/Fe_2O_3/PVA composite hydrogel	28.7 ± 0.6[a]	83.5 ± 0.2[a]	1.7 ± 0.1[a]
the pure PVA hydrogel	26.3 ± 0.3	79.7 ± 0.7	1.3 ± 0.1

[a]Statistical analysis of variance, $p < 0.05$.

degradation of magnetic nanocomposite hydrogel at different time points has shown that the magnetic hydrogel formulations have relatively intermediate and slow degradation rates (Figure 4).

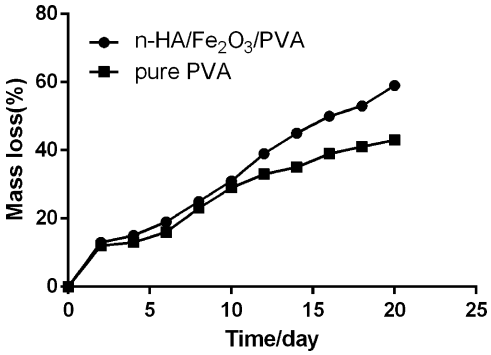

Figure 4. Degradation of the magnetic nanocomposite hydrogel at different time points. Magnetic hydrogel formulations show relatively intermediate and slow degradation rates.

3.4. Cell Compatibility. *3.4.1. Identification of the BMSCs.* To confirm the stem cell characterization for the next study, we used multilineage differentiation potential of BMSCs. We successfully characterized the differentiation capacities of rabbit (rb)-BMSCs into various lineages like chondrogenic, adipogenic, and osteogenic cells (Figure 5C–E).

3.4.2. Cell Proliferation Assay. We measured BMSC proliferation on the n-HA/Fe_2O_3/PVA composite hydrogel using the CCK-8 method (Figure 6). There was no significant difference in cell proliferation between the BMSCs cultured

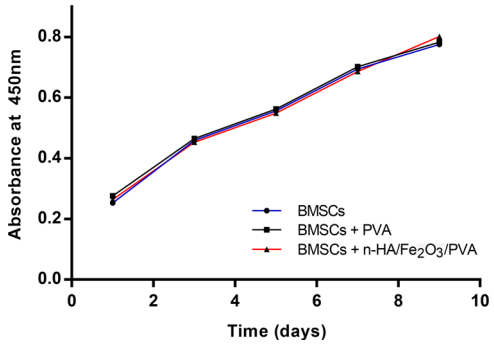

Figure 6. CCK-8 solution absorption for the group BMSCs cultured with composite gel, group BMSCs cultured with pure PVA gel, and group BMSCs cultured without hydrogel. There were no significant differences in cell proliferation.

with n-HA/Fe_2O_3/PVA composite hydrogel and either of the control groups (i.e. BMSCs cultured with pure PVA hydrogel or BMSC culture alone, $p > 0.05$).

3.4.3. Stereoscopic Optical Microscopy. After one week of BMSC culture with different forms of hydrogel, we performed stereoscopic optical microscopy. When the BMSCs were cultured with the n-HA/Fe_2O_3/PVA composite hydrogel (group A), cells had a polygon shape, contacted each other through projections, proliferated and differentiated well, and showed a regular stacking growth with time. When the BMSCs were combined with the pure PVA hydrogel, they had a polygon shape and proliferated well but we observed relatively few cells. This result shows that the magnetic nanocomposite hydrogel had better biocompatibility than pure PVA hydrogel alone.

3.4.4. SEM. According to our SEM results, when BMSCs were cultured with n-HA/Fe_2O_3/PVA composite hydrogel (group A), a large number of spindle or polygonal cells adhered to and aggregated in the pores on the gel surface. In contrast, only a small number of cells adhered to the pores on the surface of the pure PVA hydrogel (group B). This demonstrates that

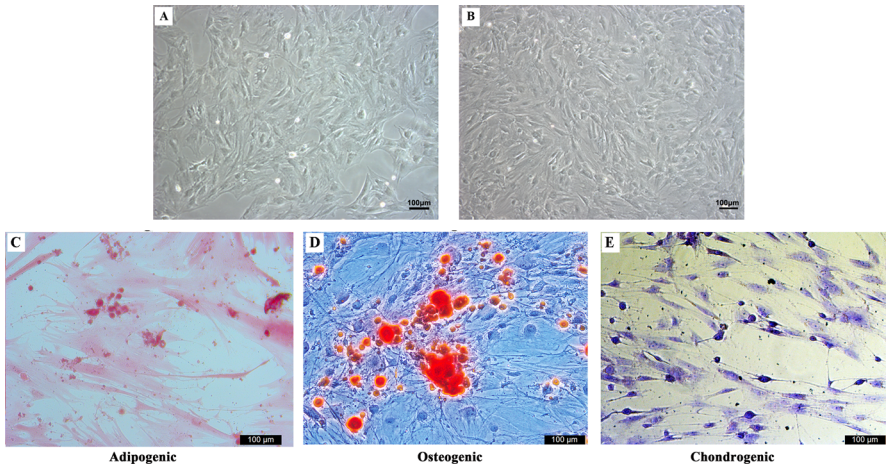

Figure 5. BMSC morphology (100×), cell adherent growth, spindle and polygonal, (A) P0, (B) P3. (C) Intracellular oil red O staining indicating lipid-rich vacuole formation of the rb-BMSCs after three weeks of adipogenic induction. (D) Alizarin red staining demonstrated that the mineralized nodules formed in the BMSCs after three weeks under the osteogenic induction. (E) After four weeks of chondrogenic induction, the cell was sectioned and stained with toluidine blue; the positive acidic proteoglycan indicated the chondrocyte-like cell formation. Scale bar = 100 μm.

DOI: 10.1021/acsomega.8b00291
ACS Omega 2018, 3, 6182–6189

the magnetic nanocomposite hydrogel had good biocompatibility with the BMSCs (Figure 7A,B).

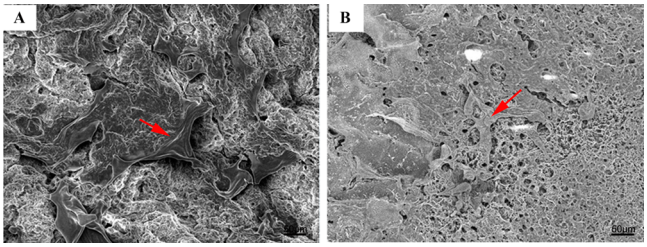

Figure 7. Hydrogel material was co-cultured with BMSCs for one week. (A) A large number of spindle or polygonal cells adhered to and aggregated in the pores on the surface of the n-HA/Fe_2O_3/PVA composite hydrogel. (B) A small number of cells adhered to the pores on the surface of the pure PVA hydrogel.

3.4.5. Photomicrographs of the Histological Findings. The BMSCs formed a capsule around the construct in the central region of the cell/scaffold constructs (Figure 8A,B). By

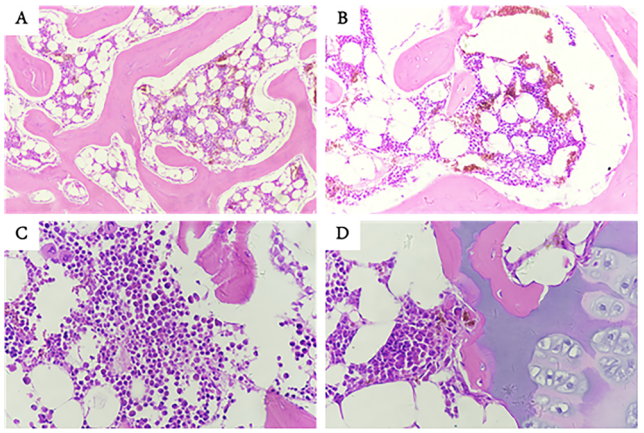

Figure 8. Photomicrographs of the histological findings in the central (A,B) and surface regions (C,D) of the cell/scaffold constructs, in static culture for 14 days (20× magnification).

contrast, at the peripheral edge of the cell/scaffold constructs, clumps of cells were found and some cells were well-dispersed. Also the cells at the surface were larger compared with those in the central region (Figure 8C,D).

The levels to enhance the immunofluorescent signal of the chondrogenic differentiation marker were obviously observed in the n-HA/Fe_2O_3/PVA composite hydrogel group (Figure 9).

3.4.6. Chondrogenic Differentiation Potential of Hydrogel Material. BMSCs cultured with the n-HA/Fe_2O_3/PVA composite hydrogel exhibited significantly higher SOX9, aggrecan, and type II collagen expression (Figure 10). This material significantly enhances the expression of cartilage-specific gene markers such as type II collagen, aggrecan, and SOX9 relative to pure PVA hydrogel during the culture period, thereby inducing differentiation of BMSCs into hyaline chondrogenic cells. In conclusion, we demonstrated that our magnetic nanocomposite hydrogel scaffold material promotes chondrogenic differentiation. Thus, the magnetic nanocomposite hydrogel may be a reliable scaffold for cartilage tissue engineering. In addition, this study will advance the development of magnetic strategies in tissue engineering to repair the damaged cartilage tissue.

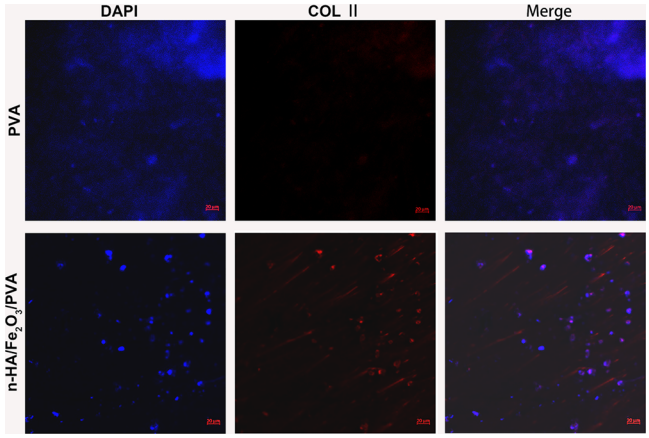

Figure 9. Confocal images of cells immunostaining of collagen type II antibody; cell nuclei were labeled with DAPI (blue) (scale bar is 20 μm).

4. DISCUSSION AND CONCLUSION

At present, the biomaterials studied in cartilage tissue engineering mainly include natural or synthetic polymers, injectable hydrogels, or other scaffold materials. A clinically useful scaffold material for cartilage tissue engineering will have good biocompatibility, biodegradability, low cytotoxicity, and certain mechanical properties.[16] The scaffold material acts as an exogenous cell carrier, namely, it promotes the migration, adhesion, proliferation, and differentiation of BMSCs, or provides structural support. In this study, we describe a novel magnetic nanocomposite hydrogel prepared using the repeated freeze−thaw approach. The aqueous solution of the composite material formed physical cross-linking points in the form of tiny crystalline regions via intermolecular H-bonds in the process of repeated freezing and thawing, which then formed a hydrogel with a three-dimensional network structure with considerable mechanical strength and ability to swell. No harmful chemicals were added throughout the process, and the biocompatibility of the composite material was not reduced. Our novel hydrogel also has high water content and good elasticity and can be prepared quickly and easily.[17]

Water content is an important property of hydrogels. In the hydrogel system, water content has a direct effect on the viscoelasticity and mechanical properties of the material. A hydrogel's compressive strength, tensile strength, and modulus increase with decreasing water content. When the water content is 80%, the tensile strength is similar to natural cartilage. When the water content is less than 80%, the homogeneity of the hydrogel becomes problematic.[18] The water content of the magnetic nanocomposite hydrogel prepared in this study was 82.6%, slightly less than the water content of the pure PVA hydrogel (85.3%, Figure 3). During hydrogel formation, the molecular chains in the amorphous region unwrap and the lamellar structure in the crystalline region begins to expand. This expansion is accompanied by the turnover and sliding of molecular chains, a process that absorbs the energy generated by the viscoelastic deformation. Therefore, high crystallinity can be compatible with high elastic modulus and elongation at break. Changes to the crystallinity of a hydrogel can indirectly suggest that its structure has changed.[19] Table 2 shows that the crystallinity of the n-HA/Fe_2O_3/PVA composite hydrogel is lower than that of the pure PVA hydrogel, indicating that adding n-HA and Fe_2O_3 reduced

DOI: 10.1021/acsomega.8b00291
ACS Omega 2018, 3, 6182−6189

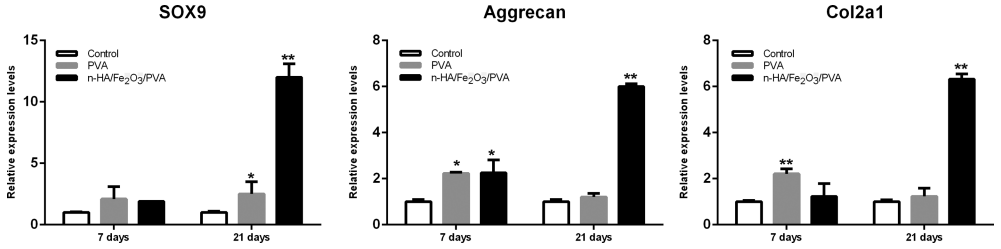

Figure 10. n-HA/Fe_2O_3/PVA enhances messenger RNA (mRNA) expression of chondrogenic markers of BMSCs. Relative levels of type II collagen (COL2A1), aggrecan (AGG), and SOX9 mRNA were determined by quantitative real-time PCR in relation to GAPDH. Data were presented as means ± standard deviations. Statistical analyses were performed using analysis of variance (Dunnett's test); $^{**}p < 0.01$, $^{*}p < 0.05$ vs ctrl (control; BMSCs cultured in maintenance medium).

the entanglement points of interchain and intrachain hydrogen bonds formed in the PVA hydrogel. While crystallinity decreased, the structure of amorphous region increased and the network structure of the PVA hydrogel became loose, thus the network gap in unit volume increased, resulting in lower crystallinity of the PVA hydrogel.[20]

Mechanical testing showed that the mechanical properties of the n-HA/Fe_2O_3/PVA composite hydrogel were superior to the pure PVA hydrogel. This may be caused by the addition of n-HA and Fe_2O_3 to the PVA hydrogel, as n-HA enhanced the mechanical properties of the composite hydrogel while promoting the repair of subchondral bone. SEM showed that many pores of different sizes were distributed on the surface of the n-HA/Fe_2O_3/PVA composite hydrogel, forming rough bumps on the surface. These structures were beneficial to the adhesion and growth of cells on the surface of the composite hydrogel, and the pores may have improved the transmission and metabolism of nutrients. When the third-generation BMSCs were co-cultured with the n-HA/Fe_2O_3/PVA composite hydrogel, we found that the cells were polygon-shaped, contacted each other through projections, and showed regular stacking growth with time. Additionally, proliferation, survival, and differentiation rates were high in BMSCs co-cultured with the composite hydrogel. A large number of spindle or polygonal cells adhered to and aggregated in the pores on the surface of the n-HA/Fe_2O_3/PVA composite hydrogel, showing that the n-HA/Fe_2O_3/PVA composite hydrogel had good biocompatibility. Moreover, the prepared n-HA/Fe_2O_3/PVA composite hydrogel showed an improvement in the differentiation of the BMSCs.

Cartilage tissue engineers have always aimed to develop novel scaffold materials with adequate mechanical strength, high biocompatibility, and hydrophilicity, which are easy to degrade and absorb. The scaffold material we describe in this study not only had all of the above characteristics but also had featured superparamagnetic nanoparticle Fe_2O_3, which can promote the proliferation and differentiation of the BMSCs and closely bind to the cell surface.

In this experiment, a novel magnetic nanocomposite hydrogel scaffold material was prepared. This hydrogel had similar water content as natural cartilage and low crystallinity. This scaffold material had good mechanical properties, and SEM demonstrated that micropores on the hydrogel surface were beneficial to the growth and proliferation of cells. In addition, experiments where BMSCs were cultured with the magnetic nanocomposite hydrogel scaffold material demonstrated that the scaffold material had good cell compatibility and induced BMSC differentiation into chondrocytes. Thus, this scaffold material has the potential for a broad range of therapeutic applications and can be considered as a promising material for cartilage tissue engineering.

AUTHOR INFORMATION

Corresponding Authors

*E-mail: jianyixiong@126.com. Phone: 86-0755-83366388. Fax: 86-0755-83356952 (J.X.).

*E-mail: dapingwang1963@qq.com. Phone: 86-0755-83366388. Fax: 86-0755-83356952 (D.W.).

ORCID

Jianghong Huang: 0000-0002-8168-0081

Notes

The authors declare no competing financial interest.

ACKNOWLEDGMENTS

This study was mainly supported by grants from Guangdong Province Science and Technology Project (grant nos. 2017A020215116 and 2015A030401017), Shenzhen R&D funding project (grant nos. JCYJ20160301111338144, JCYJ20170306092315034, and JCYJ20160429185235132), Guangdong Province Medical Research Fund Project (grant no. A2017189), and fund for high-level medical discipline construction of Shenzhen University (grant no. 2016031638).

REFERENCES

(1) Seidlits, S. K.; Khaing, Z Z.; et al. The effects of hyaluronic acid hydrogels with tunable mechanical properties on neural progenitor cell differentiation. *Biomaterials* **2010**, *31*, 3930−3940.

(2) Pourjavadi, A.; Kurdtabar, M. Collagen-based highly porous hydrogel without any porogen: synthesis and characteristics. *Eur. Polym. J.* **2007**, *43*, 877−889.

(3) Park, J.-S.; Kim, H.-A.; Choi, J.-B.; et al. Effects of annealing and the addition of PEG on the PVA based hydrogel by gamma ray. *Radiat. Phys. Chem.* **2012**, *81*, 857−860.

(4) Holloway, J. L.; Lowman, A. M.; Palmese, G. R. The role of crystallization and phase separation in the formation of physically cross-linked PVA hydrogels. *Soft Matter* **2013**, *9*, 826−833.

(5) Bock, N.; Riminucci, A.; Dionigi, C.; et al. Novel Route in Bone Tissue Engineering: Magnetic Biomimetic Scaffolds. *Acta Biomater.* **2010**, *6*, 786−796.

(6) Kobayashi, T.; Ochi, M.; Yanada, S.; et al. Augmentation of Degenerated Human Cartilage in Vitro Using Magnetically Labeled Mesenchymal Stem Cells and an External Magnetic Device. *Arthroscopy* **2009**, *25*, 1435−1441.

(7) Mayer-Wagner, S.; Passberger, A.; Sievers, B.; et al. Effects of Low Frequency Electromagnetic Fields on the Chondrogenic Differentiation of Human Mesenchymal Stem Cells. *Bioelectromagnetics* **2011**, *32*, 283−290.

(8) Ngadiman, N. H. A.; et al. γ-Fe_2O_3 nanoparticles filled polyvinyl alcohol as potential biomaterial for tissue engineering scaffold. *J. Mech. Behav. Biomed. Mater.* **2015**, *49*, 90−104.

DOI: 10.1021/acsomega.8b00291
ACS Omega 2018, 3, 6182−6189

(9) Ngadiman, N. H. A.; et al. Development of highly porous biodegradable gamma- Fe_2O_3/polyvinyl alcohol nanofiber mats using electrospinning process for biomedical application. *Mater. Sci. Eng., C* **2017**, *70*, 520−534.
(10) Sheikh, F. A.; et al. Synthesis of poly(vinyl alcohol) (PVA) nanofibers incorporating hydroxyapatite nanoparticles as future implant materials. *Macromol. Res.* **2010**, *18*, 59−66.
(11) Nazempour, A.; Van Wie, B. J. Chondrocytes, mesenchymal stem sells, and their combination in articular cartilage regenerative medicine. *Ann. Biomed. Eng.* **2016**, *44*, 1325−1354.
(12) Zhang, N.; Lock, J.; Sallee, A.; Liu, H. Magnetic Nanocomposite Hydrogel for Potential Cartilage Tissue Engineering: Synthesis, Characterization, and Cytocompatibility with Bone Marrow Derived Mesenchymal Stem Cells. *ACS Appl. Mater. Interfaces* **2015**, *7*, 20987−20998.
(13) Cao, Y.; Xiong, D.; Wang, K.; et al. Semi-degradable porous poly (vinyl alcohol) hydrogel scaffold for cartilage repair: Evaluation of the initial and cell-cultured tribological properties. *J. Mech. Behav. Biomed. Mater.* **2017**, *68*, 163−172.
(14) Osaheni, A. O.; Finkelstein, E. B.; Mather, P. T.; et al. Synthesis and characterization of a zwitterionic hydrogel blend with low coefficient of friction. *Acta Biomater.* **2016**, *46*, 245−255.
(15) Liu, Y.; Geever, L. M.; Kennedy, J. E.; Higginbotham, C. L.; et al. Thermal behavior and mechanical properties of physically crosslinked PVA/Gelatin hydrogels. *J. Mech. Behav. Biomed. Mater.* **2010**, *3*, 203−209.
(16) Bentley, G.; Bhamra, J. S.; Gikas, P. D.; et al. Repair of osteochondral defects in joints-how to achieve success. *Injury* **2013**, *1*, S3−S10.
(17) Rui-Hong, X.; Peng-Gang, R.; Jian, H.; et al. Preparation and properties of graphene oxide-regenerated cellulose/polyvinyl alcohol hydrogel with pH-sensitive behavior. *Carbohydr. Polym.* **2016**, *138*, 222−228.
(18) Choi, J.; Kung, H. J.; Macias, C. E.; et al. Highly lubricious poly(vinyl alcohol)- poly(acrylic acid) hydrogels. *J. Biomed. Mater. Res., Part B* **2012**, *100*, 524−532.
(19) Islam, A.; Yasin, T.; Gull, N.; et al. Fabrication and performance characteristics of tough hydrogel scaffolds based on biocompatible polymers. *Int. J. Biol. Macromol.* **2016**, *92*, 1−10.
(20) Zhang, F.; Wu, J.; Kang, D.; et al. Development of a complex hydrogel of hyaluronan and PVA embedded with silver nanoparticles and its facile studies on Escherichia coli. *J. Biomater. Sci., Polym. Ed.* **2013**, *24*, 1410−1425.

DOI: 10.1021/acsomega.8b00291
ACS Omega 2018, 3, 6182−6189